Variability of the Southwestern Patagonia (51°S) Winds in the Recent (1980–2020) Period: Implications for Past Wind Reconstructions

Carolina Gómez-Fontealba, Valentina Flores-Aqueveque, Stéphane Christophe Alfaro

atmosphere

MDPI

Article

Variability of the Southwestern Patagonia (51°S) Winds in the Recent (1980–2020) Period: Implications for Past Wind Reconstructions

Carolina Gómez-Fontealba [1,2,3,*], Valentina Flores-Aqueveque [1,2,3] and Stéphane Christophe Alfaro [4]

[1] Departamento de Geología, Facultad de Ciencias Físicas y Matemáticas, Universidad de Chile, Santiago 8320000, Chile; vfloresa@uchile.cl
[2] South American Dust Initiative (SANDI), Facultad de Ciencias Físicas y Matemáticas, Universidad de Chile, Santiago 8320000, Chile
[3] Millennium Nucleus Paleoclimate, Agencia Nacional de Investigación y Desarrollo (ANID) Millennium Science Initiative, Ñuñoa 7750000, Chile
[4] Université de Paris Est Créteil and Université de Paris, CNRS, LISA, F-94010 Créteil, France; stephane.alfaro@lisa.ipsl.fr
* Correspondence: carolina.gomez.f@ug.uchile.cl; Tel.: +56-942-688-310

Abstract: The Southern Hemisphere Westerly Winds (SWW) control the amount and latitudinal distribution of rainfall in southwestern Patagonia. Recent studies have shown that SWW has intensified in the last decades, but their past behavior is not yet well understood. To understand this behavior, it is necessary to analyze climatic data from meteorological stations and reconstruct their variability through paleoclimatic evidence, such as lake cores. Nevertheless, Patagonia is an austral region characterized by its complex topography and quasi lack of a meteorological network. In this work, three reanalyses are studied (MERRA-2, ERA5, and GLDAS) and compared with the Cerro Castillo and Teniente Gallardo stations (~51°S), with the aim of simulating the winds in the past. The results indicate that ERA5 and MERRA-2 simulate well the wind variability in the study region, while GLDAS is less reliable. Therefore, the first two reanalyses could be used to extend the time series of the meteorological station and calibrate a new wind proxy based on the abundance and size of the aeolian particles, reconstructing in a direct way the intensity of the SWW in the past over southwestern Patagonia.

Keywords: SWW; ERA5; MERRA-2; southwestern Patagonia

Citation: Gómez-Fontealba, C.; Flores-Aqueveque, V.; Alfaro, S.C. Variability of the Southwestern Patagonia (51°S) Winds in the Recent (1980–2020) Period: Implications for Past Wind Reconstructions. *Atmosphere* **2022**, *13*, 206. https://doi.org/10.3390/atmos13020206

Academic Editors: Rui Salgado, Maria José Monteiro, Mariana Bernardino, David Carvalho, Flavio T. Couto, Rita M. Cardoso, João P. A. Martins and Joao Carlos Andrade dos Santos

Received: 24 December 2021
Accepted: 26 January 2022
Published: 27 January 2022

1. Introduction

Southern Westerly Winds (SWW) are a belt of winds that blow from west to east at mid-latitudes due to global atmospheric circulation. Several studies have shown that these winds have recently changed in intensity and latitudinal position (e.g., [1–3]) thereby significantly impacting the climate of southern Patagonia. Indeed, the SWW control precipitations and climate [1,4], thus important variations in these winds generate environmental, social, and economic consequences over this part of the Southern Hemisphere (SH).

The behavior of SWW is currently well understood [4], but this is not case for its past variations. Due to the influence exerted by the SWW on the climate, it is fundamental to understand what controls their changes and how these winds have changed over time based on paleoclimatic evidence. Also, if you want to understand future global climate patterns, past behavior of SWW is also required, for example, to evaluate the consequences of these winds in the future atmospheric CO_2 [5]. In this sense, it is important to know the behavior of the SWW in the past, and Chile presents a unique location for reconstruction because it is the only continental mass that covers the entire latitudinal range of the SWW.

For the reconstruction of the temporal variability of the SWW, an indirect source of climate information comes from lakes cores, which have been shown to provide valuable

climate information in this region through the use of proxy records [6]. Among these, the mineral particles eroded by the wind, transported and deposited into water (lakes or sea) constitute an ideal tool for the reconstruction of past winds (e.g., [7–9]). Indeed, the characteristics (quantity, size distribution) of the particles retrieved in the laminated sediments depend directly on the frequency and strength of the winds above the threshold (u*t) of erosion, since the strongest winds are capable of transport these sediments on the surface [10].

However, before being exploitable quantitatively any proxy record must be calibrated against accurate environmental data. In a region with very few and quite recently-established meteorological stations, continuous long-term direct measurements are lacking for this calibration. Provided their quality has first been evaluated by comparison with the existing measurements, the products of different reanalyses could provide these missing calibration tools.

Indeed, of the different data sources available (e.g., meteorological stations, reanalyses, or models), reanalysis is one of the most widely used methods for studying climate variables. Reanalysis is the process whereby an unchanging data assimilation system is used to provide a consistent reprocessing of meteorological observations, typically spanning an extended segment of the historical data record. The products from a reanalysis include many variables such as wind speeds, temperature, atmospheric pressure, among others, and have not only become a staple of the atmospheric research community but are used increasingly for climate monitoring as well as for business applications in, for example, energy and agriculture [11].

An important advantage of the reanalysis is that their products are generally open-access, globally available, and continuously updated over the decades, increasing their temporal and spatial resolution [12], reducing biases, and improving possible system limitations. Examples of these updates are the replacement of the MERRA reanalysis by MERRA-2 of the Global Modelling and Assimilation Office (GMAO) [11] and the replacement of the popular ERA-Interim reanalysis by ERA5 produced by European Centre for Medium-Range Weather Forecast Reanalysis (ECMWF) [13].

In this work, the ability of three reanalyses (MERRA-2, ERA5, and GLDAS) to represent the surface wind in southern Patagonia is studied. The main objective is to analyze the variability over the last decades of the strong winds in the present-day core of the SWW (51°S). To this, the degree of agreement between the surface winds of the reanalyses and direct measurements of the few meteorological stations available in the area of study is first evaluated. In a second step, the reanalyses that best fit the data will be used to extend the time series of meteorological data in the past beyond the implementation of the meteorological stations, which will make it possible to analyze the wind variability on wider (monthly to interdecadal) timescale.

This paper is organized as follows. The next section (Section 2) describes the SWW and the area of study, the methodology, and the datasets used. Section 3 shows the time series of meteorological stations and reanalysis data. It also shows the results of the temporal variability of strong winds determined from statistical analysis. This information is used in Section 4 to discuss the consistency of the different reanalyses and to analyze the variability of the wind. Finally, the last section summarizes the results and presents the main conclusions of this work.

2. Materials and Methods

2.1. Present Day SWW over Southern Patagonia

Patagonia is a large and diverse region in southern South America that extends from ~40°S down to the southern tip of the continent (55°S). Western Patagonia features a temperate, hyper humid climate, a modest seasonal cycle, and annual mean precipitation ranging between 5000 and 10,000 mm [3]. This region faces the strong SWW, which are the prevailing winds at the mid-latitudes of the SH. These winds roughly cover the region between 30° and 70°S, and currently present a core of stronger winds centered at ~51°S [14].

These winds are responsible for the heat transport from the mid-latitudes towards the poles following undulating stationary paths [5]. Because of the topography of southern Patagonia, SWWs control the cloud cover and rainfall on the leeside of the Andes, which means that the cloud cover is strongly correlated wind speed (supplementary materials Figure S1) on the western side of the Andes [15,16].

Present day, SWW behavior is very well understood. This belt is characterized by a remarkable seasonality mainly driven by changes in sea surface temperature (SST) and atmospheric temperature gradients [17]. In austral summer (DJF), the SWW are more intense and move towards the pole reaching a maximum over ~50°S [1,18]. Conversely, in austral winter (JJA) the intensity in the core of the SWW weaken and this belt moves towards the equator expanding as far as central Chile (33–40°S) [18].

During the past few decades, the SWW belt has shown a southward shift together with an increase in the core strength (e.g., [2–4,18–21]) related to the shift to an increasingly positive phase of the Southern Annular Mode (SAM) [1,22–24] as response to changes in stratospheric ozone and greenhouse forcing [23,25,26].

This trend has been also observed in several model projections for the 21st century, which highlight the tendency to a poleward shift and an intensification of the SWW related to the current scenario of global warming (e.g., [26–28]).

Due to the behavioral changes observed in the SWW belt in recent times and its crucial influence on the climate of southern Patagonia, it is necessary to expand our knowledge about the variability of this wind belt over time.

Motivated by this, we have selected for this work three meteorological stations located in the core of the SWW (~51°S) at southwestern Patagonia, and three reanalyses (Figure 1), in order to analyze wind speed variability at different (monthly, seasonal and annual) timescales. The meteorological stations are Torres del Paine, Teniente Gallardo, and Cerro Castillo, and reanalyses chosen are MERRA-2, ERA5 and GLDAS.

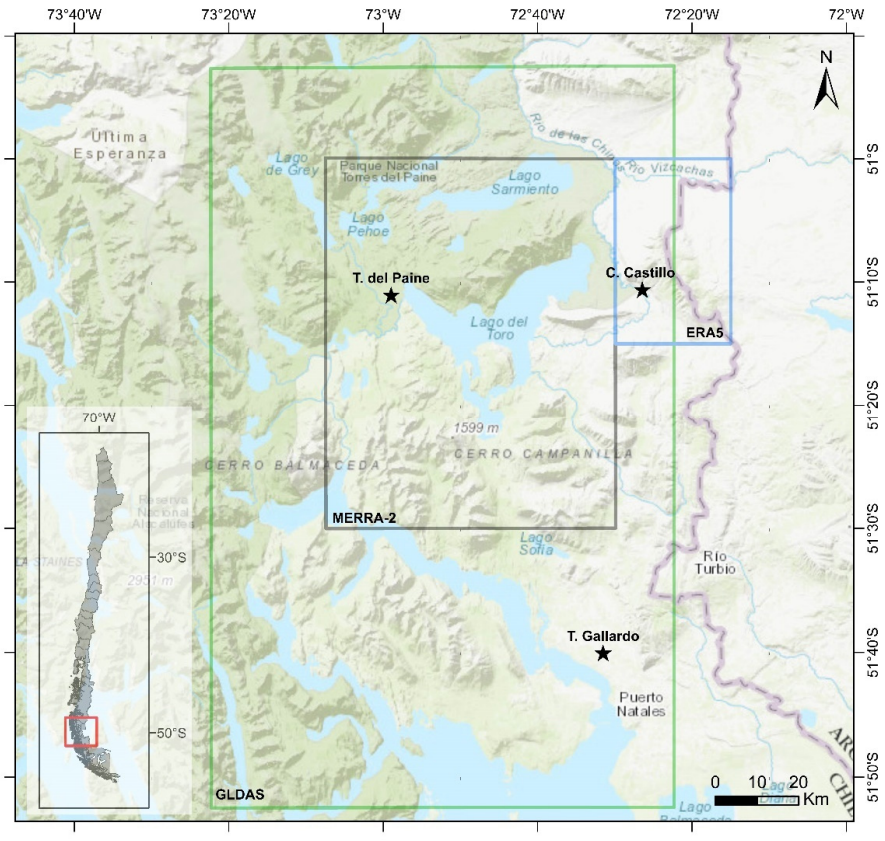

Figure 1. Location of the meteorological stations and reanalyses selected for this work. Black stars represent the meteorological stations, blue grid corresponds to ERA5 analyzed coordinates, gray grid represents data of MERRA-2, and green grid data of GLDAS (Base map from Esri).

2.2. Available Data

2.2.1. Direct Observations

In the study area there are only three meteorological stations with open access records of near-surface wind speed: Teniente Gallardo, Cerro Castillo, and Torres del Paine. Information on these stations and limits of their periods of measurements is provided in Table 1 and Figure 2. The data of the first station were obtained from the Dirección Meteorológica de Chile (DMC) (https://www.meteochile.cl/, accessed on 20 April 2021). The data for the second station were obtained from Instituto de Investigaciones Agropecuarias (INIA) (https://agrometeorologia.cl/, accessed on 20 April 2021). Finally, the data from the Torres del Paine station were facilitated by Dirección General de Aguas (DGA) (https://dga.mop.gob.cl/, accessed on 20 April 2021). At the latter station, the measurements were performed manually for a short duration and are not continued. Therefore, they will not be used in this work. The datasets of the other two stations become more complete after the hourly measurements were automated in 2016. Thus, five years of hourly measurements at the Cerro Castillo and Teniente Gallardo stations are available for validating the wind from reanalyses.

Table 1. Information and details of the meteorological station datasets.

Meteorological Station	Lat. (°)	Long. (°)	Altitude (m.a.s.l)	Temporal Resolution	Source
Teniente Gallardo	−51.66	−72.52	69	Hourly (12:00–20:00 before 2016)	DMC
Cerro Castillo	−51.17	−72.43	115	Hourly	INIA
Torres del Paine	−51.18	−72.98	25	Hourly	DGA

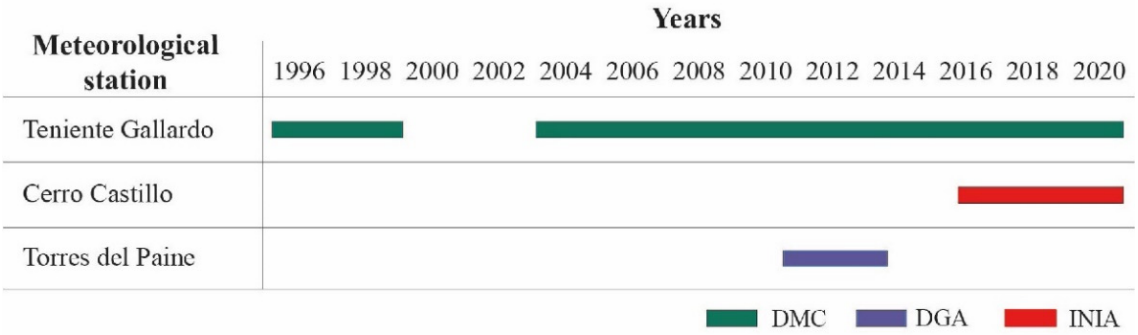

Figure 2. Periods of measurements at different meteorological stations. The data obtained from DMC is presented in green, the data obtained from DGA in blue, and the data facilitated by INIA in red.

Although short, these historical records are important as they serve to validate the data series of the reanalysis used in this work.

2.2.2. Reanalysis Data

The behavior of large-scale winds was studied through three atmospheric reanalyses: (1) the European Centre for Medium-Range Weather Forecast Reanalysis (ERA5) [13], (2) Version 2 of the Modern-Era Retrospective analysis for Research and Applications (MERRA-2) [11], and (3) the Global Land Data Assimilation System (GLDAS) [29].

ERA5 is the fifth generation of atmospheric reanalysis produced by European Centre for Medium-Range Weather Forecast Reanalysis (ECMWF). It replaces the very popular ERA-Interim reanalysis, which was progressively becoming outdated and was stopped at the end of August 2019. ERA5 provides hourly data and time series extending from the year 1950 to present time with a high horizontal resolution of 0.25° x 0.25° (Table 2) [13]. However, the data from 1950 to 1979 were not used because the corresponded to a preliminary version of ERA5 when we carried out this study (the final version is expected to become

available towards the end of 2021 [30]). Data were downloaded from the Copernicus Climate Data Store (https://cds.climate.copernicus.eu/, accessed on 30 April 2021).

Table 2. Summary of the reanalysis datasets used in this work.

Reanalysis	Period Covered	Temporal Resolution	Spatial Resolution	Reference
ERA5	1979–2020	Hourly	0.25° × 0.25°	Hersbach et al. (2020)
MERRA-2	1980–2020	Hourly	0.5° × 0.625°	Gelaro et al. (2017)
GLDAS	1948–2014	Daily	1.0° × 1.0°	Rodell et al. (2004)

MERRA-2 of the Global Modelling and Assimilation Office (GMAO 2015) is an up-to-date reanalysis for the satellite era (from 1980 onward). The spatial resolution of the model is 0.5° latitude x 0.625° longitude [11] and provides data series with hourly temporal resolution (Table 2). The datasets, corresponding to near-surface (10 m above ground), wind speed were extracted using the Giovanni NASA interface (https://giovanni.gsfc.nasa.gov/, accessed on 20 April 2021).

GLDAS is a system jointly developed by scientists at the National Aeronautics and Space Administration (NASA), Goddard Space Flight Center (GSFC) and the National Oceanic and Atmospheric Administration (NOAA). The system aims to ingest satellite and ground-based observational data products and generate optimal fields of land-surface states and flows [29]. The spatial resolution is 1.0° x 1.0° with daily data for the 1948–2014 period (Table 2). These datasets are available at the NASA Goddard Earth Sciences Data and Information Services Center (GES DISC) as well as via Giovanni NASA (https://giovanni.gsfc.nasa.gov/, accessed on 20 April 2021).

2.3. Analysis of Wind Time Series

First, the coherence between the reanalyses data and the in-situ wind measurements is analyzed because possible discrepancies were expected due to the complex topography of Patagonia. High (hourly) and medium (daily) resolution data were used for the study and statistical indicators such as the frequency of occurrence of strong winds in a given month or year were calculated to quantify the high-resolution temporal variability of the regional winds. The focus was set on the strongest winds because they are those responsible for the transport of particles on the surface [10].

For evaluating the performance of the reanalysis in the study area the following time series of the grids closest to the meteorological station were chosen: (−73.125, −51.5, −72.5, −51) for MERRA-2, (−72.25, −51.25, −72.5, −51) for ERA5, and (−73.375, −51.875, −72.375, −50.875) for GLDAS (Figure 1). Observation wind time series were then compared with data measured at hourly (for MERRA-2 and ERA5) and daily (for GLDAS, MERRA-2, and ERA5) resolution. Because the GLDAS period (1948–2014) does not overlap the period recorded at the Cerro Castillo and Teniente Gallardo stations (2016–2020; Figure 2) but presents an interestingly long time series of data, its consistency with ERA5 and MERRA-2 was evaluated. To do this, statistical parameters such as the bias, root mean squared error (RMSE) and correlation coefficient (R) were used to quantify the differences between reanalyses data and in-situ wind measurements.

Finally, as indicated above, the occurrence of strong winds in the study area was studied considering that only winds above the saltation threshold (u*t) can effectively mobilize sediments (aeolian particles) over the surface [10] and are of interest for paleoclimate reconstructions. The saltation threshold depends on the size of the erodible grains [10], on the humidity of the soil [31,32], and on the roughness of the surface, itself being sensitive to the presence of non-erodible elements such as stones or vegetation [33,34]. Because the exact value of u*t is unknown for the area of study, it was arbitrarily assumed that the strong winds above an elevated percentile (e.g., 90th percentile (V90)) of the statistical distribution of the hourly and daily winds were responsible for the most significant erosion events. Then the monthly and yearly numbers of hours/days that exceeded this thresh-

old were counted and subsequently analyzed to study the variability of the wind at the meteorological stations and in the reanalyses.

3. Results

3.1. Local Wind Variability

The synchronicity of the measurements performed after 2016 at Cerro Castillo and Teniente Gallardo allows checking the consistency of the data collected at the two stations. In spite of the distance (ca. 55 km.) separating them, the time series of daily averaged winds (Figure 3a) are quite strongly correlated (R = 0.87, Figure 3b). This shows that the measurements performed at any which one of the two stations are not of purely local interest but are representative of a much larger area including the region of study. The main differences between Cerro Castillo and Teniente Gallardo are observed in the direction of the wind (Figure 3c). Even though both stations have fundamentally winds from the west, the Teniente Gallardo station has a significant north component in its measurements (Figure 3(c1)).

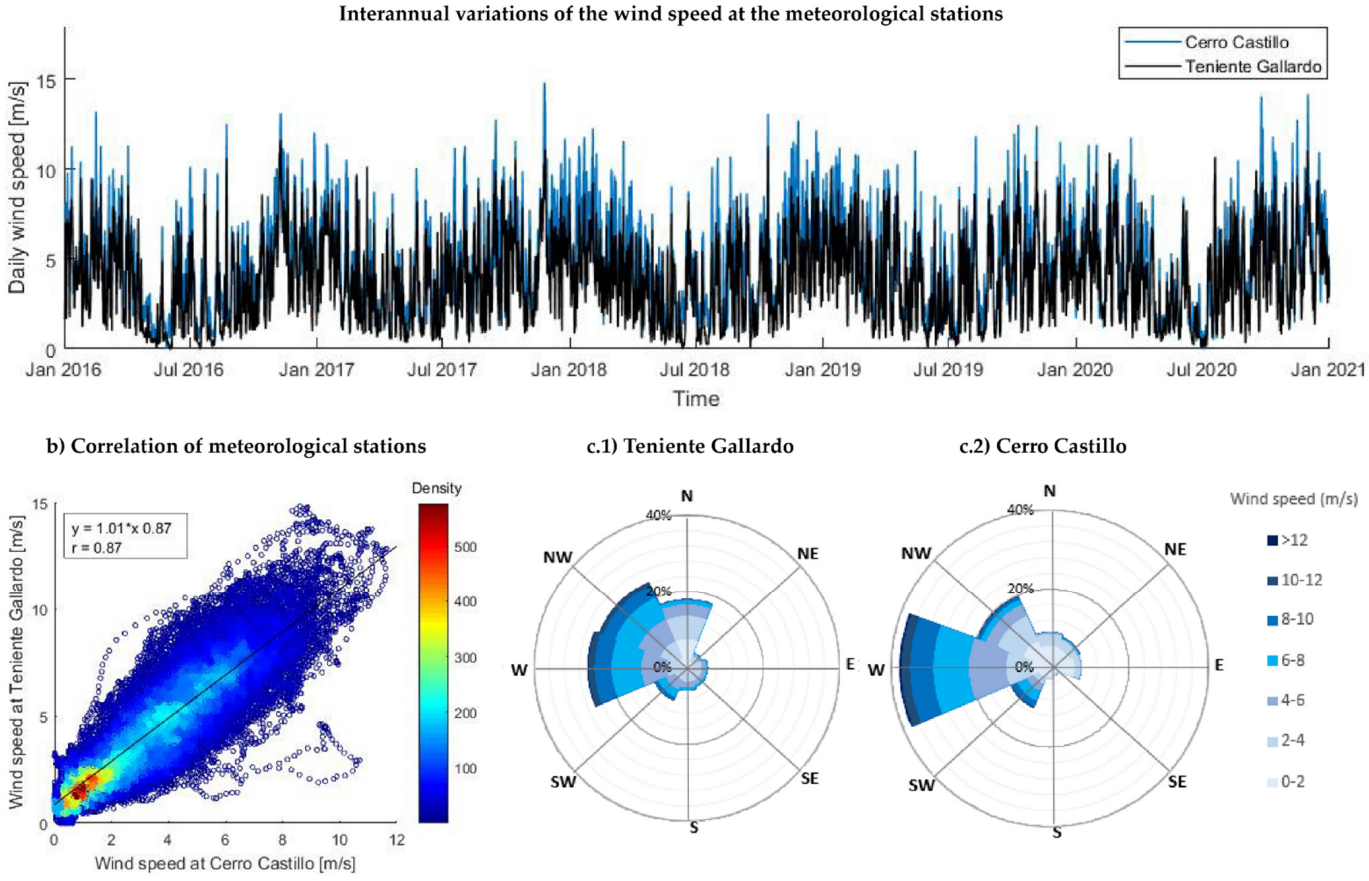

Figure 3. (**a**) Consistency of the temporal variability of the daily averages of the 10m wind recorded at Cerro Castillo and Teniente Gallardo stations. (**b**) Correlation between wind speed at Cerro Castillo and Teniente Gallardo. (**c**) Wind direction and speed frequency at the Cerro Castillo (1) and Teniente Gallardo (2) stations for the 2016–2020 period.

In the following, it was arbitrarily chosen to adopt the measurements of the Cerro Castillo station as a reference for the regional situation. The analysis of these data shows that maximum wind speed (6– >12 ms^{-1}) are mainly from the west whereas minimum speeds (0–4 ms^{-1}) come mainly from the northwest (Figure 3(c2)).

At the annual timescale, the measurements reveal a significant seasonality in wind speed characterized by strong winds during the austral summer months (December-January-February; DJF), and weak winds in the austral winter (June-July-August; JJA)

(Figure 3a). Seasonality is also observed in wind direction (Figure 4). During the austral summer and spring, the strongest winds come from the west (Figure 4a,d), whereas they come from the west and northwest during the austral fall and winter (Figure 4b,c).

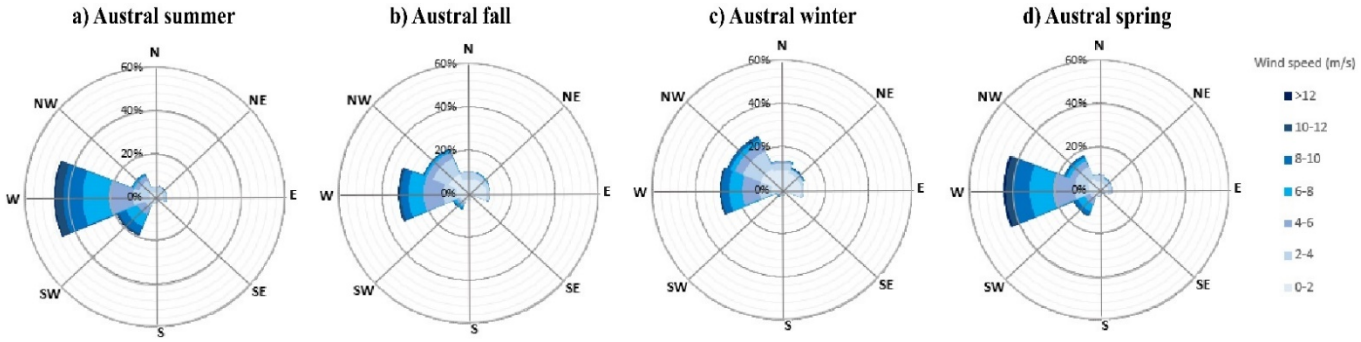

Figure 4. Seasonal variability of wind direction frequency for the period 2016–2020. (**a**) Austral summer. (**b**) Austral fall. (**c**) Austral winter. (**d**) Austral spring.

The statistical distribution of hourly winds speeds for the period 2016–2020 shows an asymmetric distribution with data shifted towards weaker winds (Figure 5a). Most of the data are concentrated between 0 and 2 ms^{-1}, while winds between 2 and 8 ms^{-1} are distributed in two main modes, one between 2 and 4 ms^{-1}, and the other between 6 and 8 ms^{-1} Finally, winds greater than 8 ms^{-1} present lower frequencies (<3%).

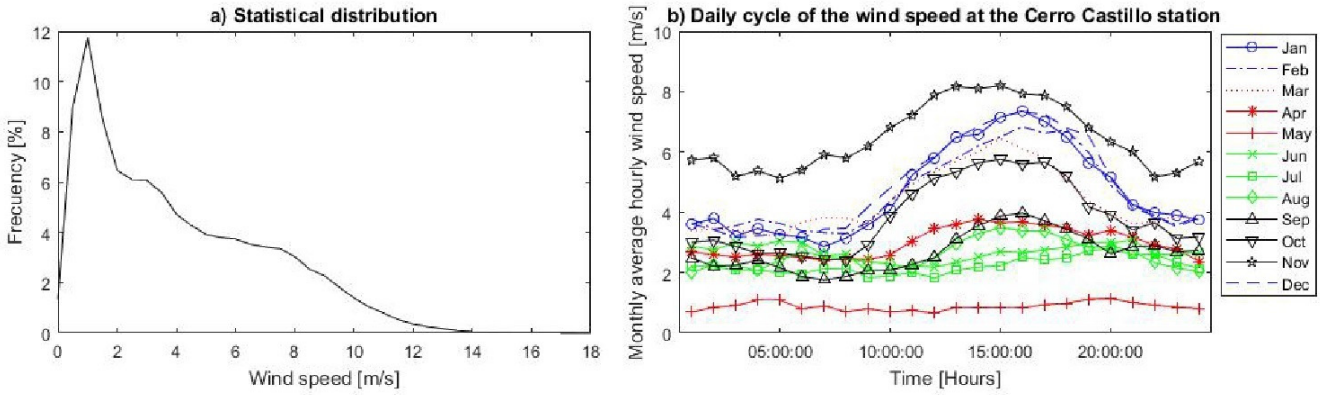

Figure 5. (**a**) Statistical distribution of the hourly winds measured between 2016 and 2020 at the Cerro Castillo station. (**b**) Hourly variation of the monthly averaged (daily cycle) of the wind speed at the Cerro Castillo station in 2016. Blue lines represent summer months (DJF), red lines correspond to fall months (MAM), green lines indicate winter months (JJA), and black lines are spring months (SON).

On a daily scale, it can be observed that winds are generally more intense during the afternoon, mainly between 12.00 a.m and 18.00 p.m, while at night, the intensity of the winds decreases (Figure 5b). This diurnal cycle was observed most of the year (except in June and July which have their maximum after 18.00 h). During the austral summer (DJF), the daily cycle is much more marked than in austral winter (JJA), when the winds are weaker and less variable (Figure 5b).

3.2. Reanalysis Validation

As indicated in Section 2.2, the validation was carried out in two steps: first, the data of the Cerro Castillo meteorological station were used to assess the quality of the MERRA-2 and ERA5 wind products, then GLDAS was compared with the other reanalyses to assess the possibility of extending the time series towards a more distant past (i.e., before 1980). Table 3 summarizes the error metrics related to the comparison between the daily wind of Cerro Castillo station and those of ERA5 and MERRA-2. Table 4 shows the parameters for the comparison between GLDAS and the other two reanalyses.

Table 3. Results of the comparison of the MERRA-2 and ERA5 daily winds with the measurements performed for 5 years (2016–2020) at the Cerro Castillo meteorological station.

	Annual			DJF			MAM			JJA			SON		
	R	**RMSE**	**Bias**	**R**	**RMSE**	**Bias**	**R**	**RMSE**	**Bias**	**R**	**RMSE**	**Bias**	**R**	**RMSE**	**Bias**
MERRA-2	0.87	2.67	2.26	0.79	2.76	2.36	0.86	2.59	2.24	0.83	2.68	2.24	0.88	2.67	2.21
ERA 5	0.88	1.87	−1.28	0.88	1.98	−1.66	0.88	1.51	−0.88	0.81	1.73	−0.89	0.89	2.20	−1.70

Table 4. Same as Table 3, but for the comparison of GLDAS with MERRA-2 and ERA5 and the 1980–2014 period.

	Annual			DJF			MAM			JJA			SON		
	R	**RMSE**	**Bias**	**R**	**RMSE**	**Bias**	**R**	**RMSE**	**Bias**	**R**	**RMSE**	**Bias**	**R**	**RMSE**	**Bias**
MERRA-2	0.47	2.62	−0.43	0.41	2.39	−0.03	0.46	2.57	−0.64	0.48	2.71	−0.93	0.44	2.77	−0.10
ERA5	0.36	4.41	−3.96	0.31	4.25	−3.81	0.3	4.40	−3.93	0.34	4.54	−4.11	0.35	4.47	−4.01
Mean	0.42	3.52	−2.20	0.36	3.32	−1.92	0.38	3.49	−2.29	0.41	3.63	−2.52	0.40	3.62	−2.06

The annual R ranging between 0.86 and 0.88, and the low associated error indicate a high level of agreement between the temporal variations of the daily wind data of both MERRA-2 and ERA5 and those of the measurements. Slightly higher correlations were observed during austral spring than in austral winter (Table 3).

Values of bias indicate that MERRA-2 tends to overestimate the in-situ wind measurement ($Bias_{ANN}$ = 2.26 ms^{-1}, Table 3), whereas ERA5 tends to slightly underestimate them ($Bias_{ANN}$ = −1.28 ms^{-1}, Table 3). As expected, the bias is slightly larger during austral summer, when the wind intensity is stronger, than during austral winter, when the intensity of the wind is lower.

The level of agreement between GLDAS and the other two reanalyses is much less satisfying (Table 4) with a mean annual R value of 0.42 and higher values of RMSE (mean $RMSE_{ANN}$ = 3.52 ms^{-1}).

In summary, these preliminary results suggest that (1) the performance of GLDAS does not compare to that of the other two reanalyses, and (2) despite the systematic negative and positive biases observed in ERA5 and MERRA-2, respectively, both reanalyses are able to represent adequately the wind variability in the region of study. In order to confirm these findings, a more detailed evaluation of the MERRA-2, and ERA5 products is proposed in the following subsections.

3.2.1. MERRA-2 vs. Cerro Castillo

Figure 6 provides an example of the comparison of the wind speed measured at the Cerro Castillo station and the MERRA-2 reanalysis. At the hourly temporal resolution (Figure 6a), the daily cycle is well represented by the reanalysis. However, the higher wind speeds fit better than the minimums, since generally the lower values are overestimated. Therefore, the positive bias of MERRA.2 ($Bias_{ANN}$ = 2.26 ms^{-1}, Table 3) can be in large part explained by this overestimation of the lower wind speeds.

At the daily resolution, the consistency of the reanalyses with the measurements appears clearly (Figure 6b). This high correlation (R = 0.87) is also observed for the entire period (Figure 7b). However, the level of agreement between the reanalysis and measurement decreases when hourly temporal resolution is considered (R = 0.73, Figure 7a).

3.2.2. ERA5 vs. Cerro Castillo

The daily covariation between the measurements and data yielded by the reanalysis are shown in Figure 8. In general, it can be observed that the reanalysis presents the same variability of wind speed as that measured at the Cerro Castillo station but with a lower amplitude, underestimating in-situ measurements most of the year ($Bias_{ANN}$ = −1.28 ms^{-1}, Table 3). During the austral summer (DJF) and spring (SON) months this difference

increases (−1.66 and −1.7 ms^{-}1, respectively, Table 3) while in fall (MAM) and austral winter (JJA) the underestimation decreases (−0.88 and −0.89 ms^{-1}, respectively, Table 3).

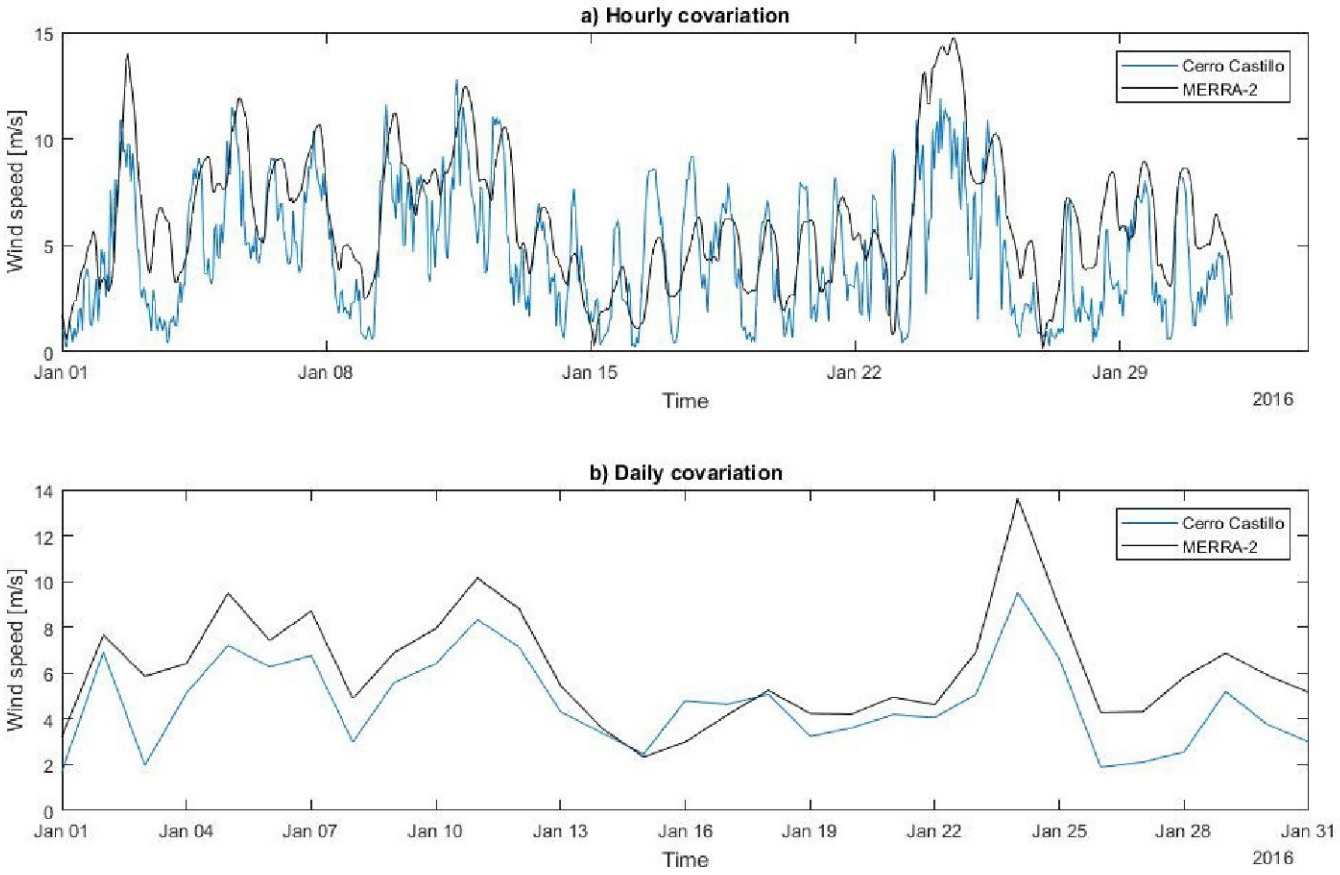

Figure 6. (**a**) Example of hourly covariation of wind speed between MERRA-2 and the Cerro Castillo station in January 2016. (**b**) Example of the covariation of the daily average wind speed between MERRA-2 and the Cerro Castillo station in January 2016.

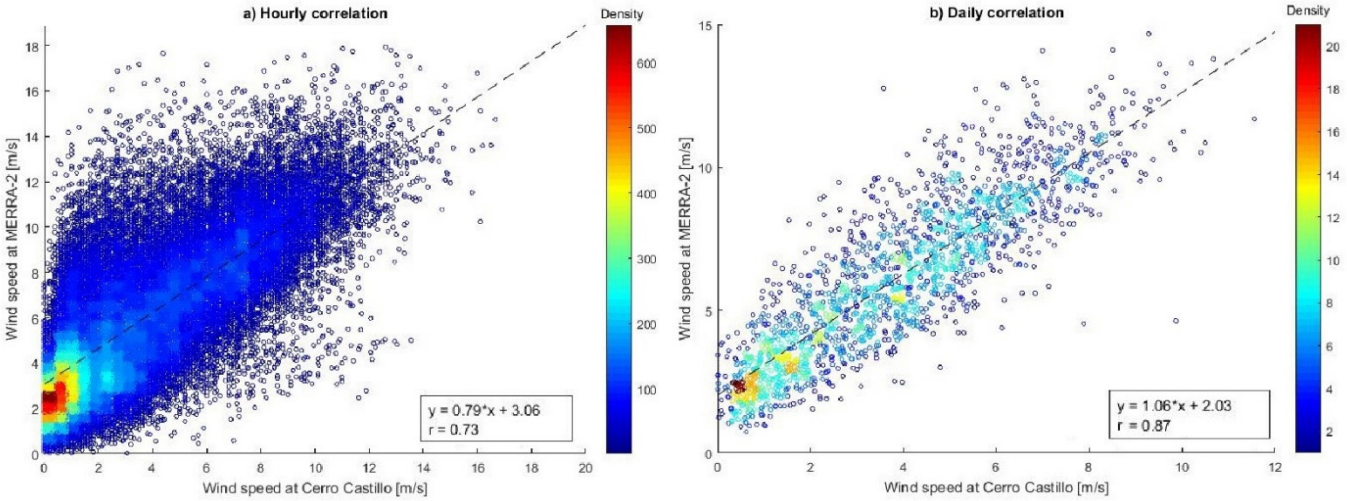

Figure 7. (**a**) Correlation between the MERRA-2 reanalyzed wind speed for the period 2016–2020 and the measurements of the Cerro Castillo station at a) hourly, and (**b**) daily temporal resolutions. The dashed lines represent the linear trend of the data.

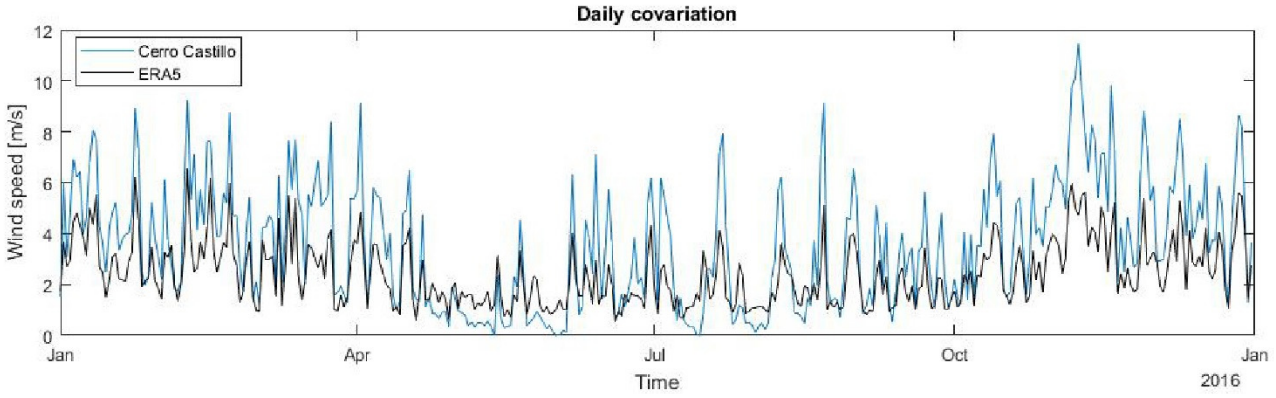

Figure 8. Daily average covariations of the wind speed measured at the Cerro Castillo station and the ERA5 data series for year 2016. The blue and black lines correspond to in-situ measurements and the reanalyzed products, respectively.

At daily time scale, the reanalysis presents a strong correlation (R_{ANN} = 0.88 and $RMSE_{ANN}$ = 1.87, Table 3) with the data measured at Cerro Castillo. This indicates that in spite of a tendency to underestimate the magnitude of the observed wind speed (slope = 0.47), its temporal variations are correctly simulated by the ERA5 reanalysis at the daily temporal resolution (Figure 9). As was already observed with MERRA-2, the agreement is less satisfying at hourly scale (data not shown).

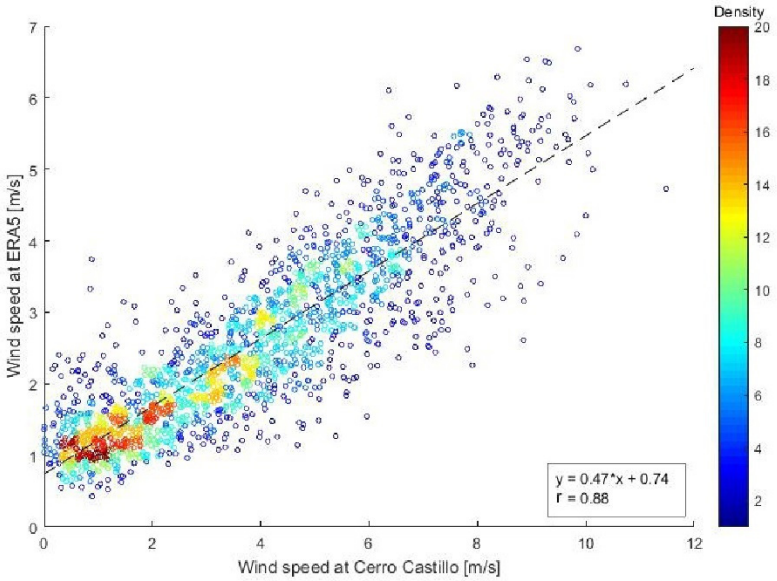

Figure 9. Daily correlation of wind speed between the Cerro Castillo station and the ERA5 reanalysis for the period 2016–2020. The dash line represents the linear trend of the data.

Summarizing, at the daily resolution wind speeds from MERRA-2 and ERA5, present similar levels of agreement (R_{ANN} = 0.86 and R_{ANN} = 0.88 respectively, Table 3) with the reference data of the Cerro Castillo station.

3.3. Ability of the Reanalyses to Simulate the Frequency of Strong Hourly Winds

As detailed in Section 2.2, strong hourly winds play an important role in wind erosion. These strong winds were arbitrarily defined as being above the 90th percentile (V90) of the statistical distribution of the hourly winds in a period of reference (2016–2020, in this study). Because of the tendency of the reanalyses to overestimate (MERRA-2) or underestimate (ERA5) the measured wind, V90 is not expected to have the same value when calculated

from the observations or from the two reanalyses. This is indeed the case (Table 5): V90 is 8.31, 4.89, and 10.6 ms^{-1} for Cerro Castillo, Era5 and MERRA-2, respectively.

Table 5. Values of V90 for the Cerro Castillo station and three reanalyses studied.

Meteorological Station/Reanalysis	Period Analyzed	Temporal Resolution	V90 (ms^{-1})
Cerro Castillo	2016–2020	Hourly	8.31
ERA5	2016–2020	Hourly	4.93
MERRA-2	2016–2020	Hourly	10.66

The monthly occurrence of strong hourly winds in MERRA-2 is similar to those observed at the meteorological station (Figure 10a). In both time series, an important seasonality characterized by strong winds during the austral summer (DJF) and weak winds in the austral winter (JJA), is observed. Data show a strong linear correlation (R = 0.883) (Figure 10b), indicating that the reanalysis simulates well the number of strong monthly winds measured at the station, despite having a higher V90 than the Cerro Castillo station (see Table 5).

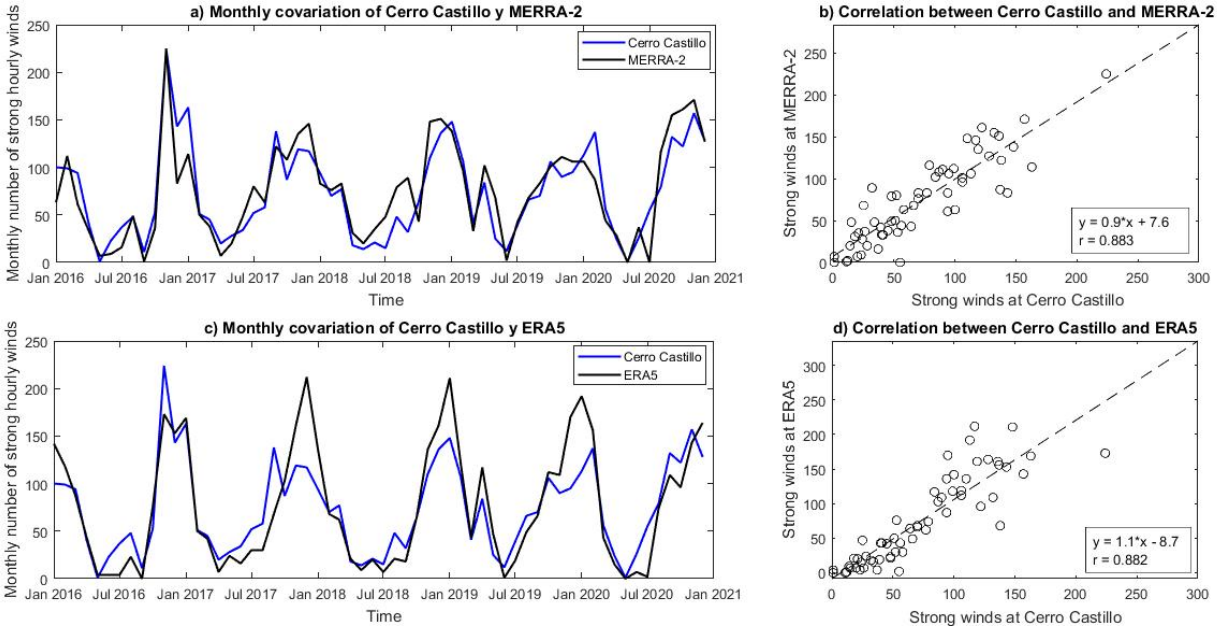

Figure 10. (**a**) Monthly number of strong hourly winds at the Cerro Castillo station and MERRA-2 between 2016 and 2020. (**b**) Correlation between the monthly number of strong winds of MERRA-2 and those observed in the period 2016–2020. (**c**) Monthly number of strong winds at hourly resolution for the Cerro Castillo station and the ERA5 between 2016 and 2020. (**d**) Correlation between the monthly numbers of strong winds at hourly resolution of ERA5 with those observed in the period 2016–2020.

Similarly, the monthly occurrences of strong hourly winds at Cerro Castillo and in the ERA5 reanalysis are in good agreement (Figure 10c). The temporal variability is the same, being characterized by intense winds occurring fundamentally in the austral summer (December and January), while during austral winter strong winds decrease to only a few hours per month. For ERA5, the level of agreement with the measurements (R = 0.882, Figure 10d) compares to that of MERRA-2 (R = 0.883, Figure 10b), indicating that the two reanalyses simulate equally well the monthly number of strong hourly winds.

Figure 11 displays for ERA5 and MERRA-2 the proportion of strong hourly winds in each year of their periods of availability. For comparison, the shorter period (2016–2020) of the Cerro Castillo measurements is also reported.

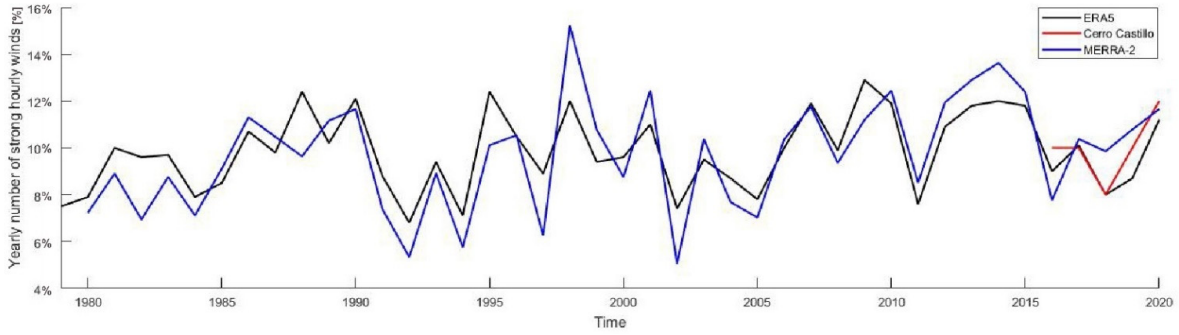

Figure 11. Yearly number of strong hourly winds from the ERA5, MERRA-2 and Cerro Castillo station for the period 1979–2020.

The data of MERRA-2 and ERA5 are consistent. The number of hours of strong winds varies between 5 and 15% (Figure 11). Interestingly, the interannual variability of the strong winds is characterized by the alternation of several years of frequent strong winds (e.g., 1986–1990; 1995–2002; 2008–2015) with calmer periods (e.g., 1992–1994; 2002–2005; 2017–2019) whose return period seems to be of the order of 10 years. Finally, both ERA5 and MERRA-2 concur on the fact that the number of yearly strong wind hours has tended to increase in the last 40 years (Figure 11).

3.4. Comparison of 'Calm' and 'Strong Winds' Years

The previous results showed that the yearly number of hours exceeding the threshold (V90) corresponding to the definition of the strong winds can vary two-fold from one year to the next. This suggests a shift of the frequency distribution of the speed of the hourly winds towards larger values during strong winds years. In other words, not only should the frequency of winds above V90 increase in some years, but their maximum velocity should also be larger in those years. This is confirmed by the excellent correlation (R_{ERA5} = 0.94 and $R_{MERRA\text{-}2}$ = 0.99) between the 95th percentile (V95) of the wind speeds in a given year and the proportion of strong winds in this year (Figure 12). V95 is only 7% larger than V90 during the calm years of the 1980–2020 period, but more than 20% above in the strong wind years.

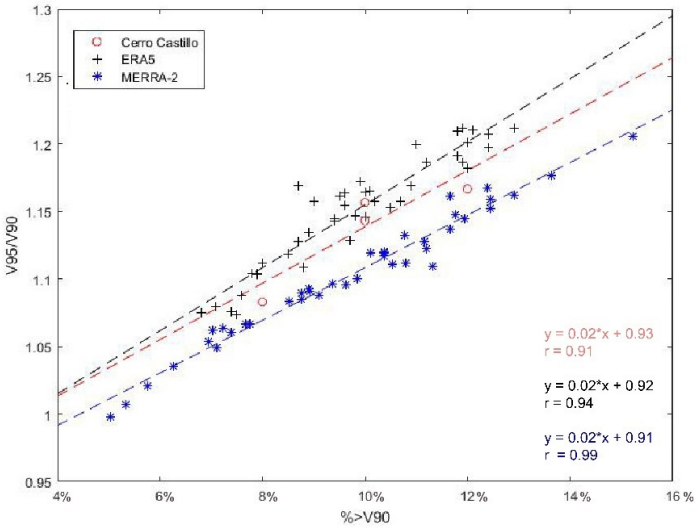

Figure 12. Evolution of the 95th percentile (V95) of the distribution of the hourly wind speeds in a year with the proportion of winds (%V90) exceeding the threshold (V90) used for defining 'strong winds', V95 was normalized by V90 to facilitate the comparison of the two reanalyses (ERA5 and MERRA-2) with the observation made at the Cerro Castillo station. The dashed lines represent the linear trend of the data.

4. Concluding Remarks

The reanalyses and the measurements have facilitated the understanding of the recent wind variability in southwestern Patagonia (51°S). The first important result is that despite the complex topography of the region of study the winds measured at the Cerro Castillo and Teniente Gallardo meteorological stations are strongly correlated. This commonality of behavior indicates that the measurements made at the stations are representative of a much larger area that their immediate vicinity.

In general, the surface winds come mainly from the west and show important seasonal variations characterized by intense winds in austral summer (DJF) and weaker winds during austral winter (JJA). This seasonality together with the predominant wind direction is consistent with previous research of the SWW in Patagonia (e.g., [1,18,35]). Measurements from meteorological stations indicate diurnal variability with strong winds occurring during the afternoon, mainly between 12.00 and 18.00 h, and weaker winds at night between 0.00 and 5.00 h, increasing these differences in the austral summer months (DJF). This pattern had already been observed previously in the area, particularly in the Patagonian steppe ~52°S (e.g., [36]). The authors of the latter study chose arbitrarily year 2008 for their analysis, and noticed that, in the daily distribution of the wind speed, the speeds were lower at night and early morning, while the highest values occurred at noon.

Regarding the ability of the three tested reanalyses to simulate the temporal variability of the daily averaged wind, two of them (ERA5 and MERRA-2) perform quite well (correlation coefficient of 0.88 and 0.87 with the observations, respectively). With R = 0.42, the third reanalysis (GLDAS) appeared as less reliable and was not retained for the rest of the study.

In terms of magnitude, the reanalyses are not expected to do as good a job as with the temporal variations. Indeed, the grid values in a reanalysis represent an average within a cell of hundreds of square kilometers, which smoothes the modeled variability [37].

This tendency towards underestimation had already been mentioned in different studies focusing on the SH. For instance, [38] reported an average wind speed underestimation of 1.18 ms^{-1} at the Southern Antarctic Peninsula, while [39] observed that ERA5 underestimates the magnitude of the wind and its standard deviation along the austral Pacific Ocean between 40° and 56°S.

For MERRA-2, the analysis showed that it adjusts well to maximum speeds but tends to overestimate the minimum speed on an hourly scale as well as the monthly average wind speed. This has been previously stated by [40] in their study carried out in the southeastern Patagonia, where they observed an overestimation of the wind speed, particularly in periods of lower speeds.

In summary, the evaluation of the consistency of the reanalyzed winds with the data of the meteorological stations on the one hand, and of ERA5 with MERRA-2 on the other hand, showed that interest of the reanalyses lies in their common ability to simulate properly the variations of the wind velocity rather than its magnitude. Moreover, the reanalysis products are available at a resolution fine enough (daily) for the long-term reconstruction of the wind erosion in the region of study.

When applied to the MERRA-2 and ERA5 (not shown) data, a wavelet spectral analysis not only confirms the importance of the seasonal and annual cycle but also of multi-annual modes of variabilities (Figure 13). For instance, a 2 to 4-year cycle clearly stands out between 1981 and 1985, or between 1992 and 2002. This periodicity could be related to the (1) influence of atmospheric event such as the Southern Annular Mode (SAM) that presents a variability on scales of 2 to 3 years [41] or (2) El Niño-Southern Oscillation (ENSO, [42]) that has variations from around 2 to 7 years (e.g., [43,44]).

Although ENSO is an atmospheric event that affects low-mid latitudes, several authors have shown that it can have an indirect effect on the climate in much of southern South America, interacting with other atmospheric events, such as the SAM (e.g., [1,14]), also known as Antarctic Oscillation (AAO, [45]). SAM develops at high latitudes, being characterized by pressure anomalies of one sign centered in the Antarctic and anomalies of the opposite sign on a circum-global band at about 40–50°S [1]. This event is directly

related to the changes in intensity and position of the westerly winds in southwestern Patagonia [1,4]. Therefore, the positive trend of the number of strong winds towards the present observed in ERA5 or MERRA-2 could be directly related to the general trend of the SAM towards a positive phase, which would be causing the increase in the speed of the winds in Patagonia (e.g., [1,4,22–24,46]).

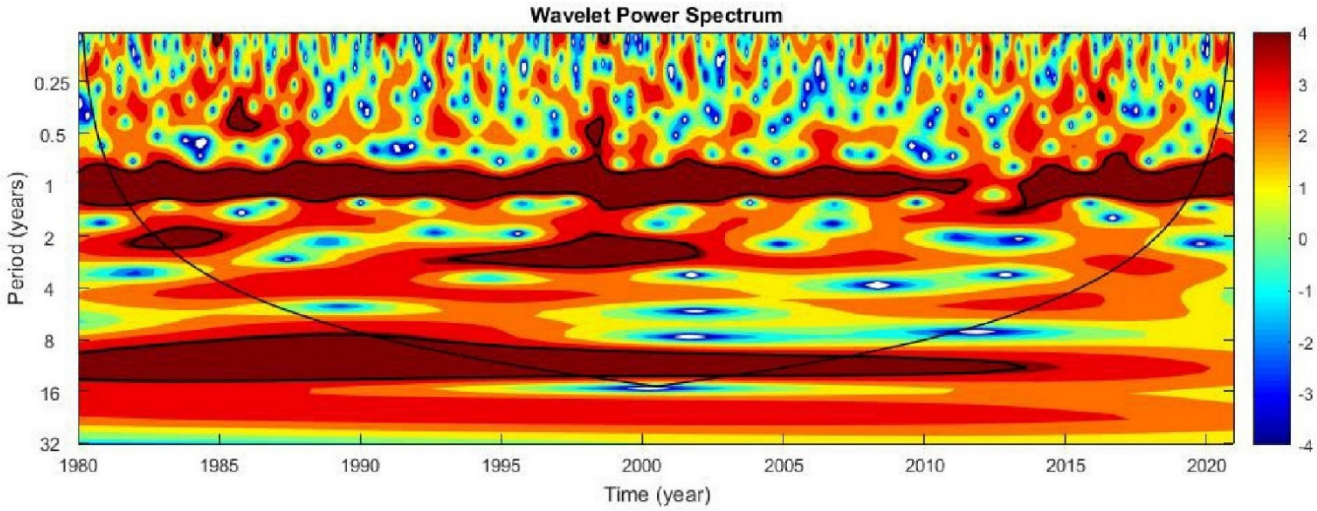

Figure 13. Wavelet power spectrum applied to MERRA-2 daily time series between 1980 and 2020. The fine black contour lines enclose regions of >95% confidence levels, and the parabola marks the cone of influence outside of which edge effects may distort results. The color bar relates the colors in the power of the spectrum.

At inter-decadal scale, 16-year frequency is observed to be particularly present between 1990 and 2006 (Figure 13). This periodicity could be related to the Pacific Decadal Oscillation (PDO, [47]), an atmospheric phenomenon that presents frequencies between 20 and 30 years [48] and plays a major role in the South American climate. This atmospheric phenomenon is described as El Niño-like, because its warm (cold) phases are very similar to El Niño (La Niña) events, although of smaller amplitude [1,49].

The combination of the pluriannual cycles has a detectable effect on the frequency of strong winds in the period 1980–2020. Periods of 2 to 4 years of reduced winds follow periods of stronger activity. Having documented precisely the limits of these periods will be precious for interpreting and calibrating quantitatively the most recent section of the sediments core recovered from lakes of the area.

Currently, lakes suitable for coring are being identified. They must meet specific conditions regarding the inputs of sediments or their preservation after deposition. For example, a closed lake without constant supply of sediment, such as from river o alluvial sediments, and exposed to wind current could guarantee a record containing a direct wind proxy that has been accumulated and preserved over time. Once calibrated, this wind proxy would allow to determine the magnitude and timing of past changes in strength experienced by SWW belt at its core (51°S) by reconstructing quantitatively the wind intensity through the characteristics (size grain and abundance) of the aeolian lithic particles.

This direct reconstruction of paleo-wind intensities from aeolian lithic particles would be a pioneering work for this region, offering the opportunity to improve substantially the previous reconstructions of the SWW based on indirect proxies such as terrigenous supply (e.g., [14,18,50,51]), changes in vegetation (e.g., [52,53]) or glacier advances (e.g., [54]).

Supplementary Materials: The following are available online at https://www.mdpi.com/article/10.3390/atmos13020206/s1, Figure S1. (a) Covariation of the wind speed of MERRA-2 and the cloud cover of the MODIS satellite. (b) Linear correlation of the wind speed of MERRA-2 and the cloud cover of the MODIS satellite.

Author Contributions: C.G.-F.: Conceptualization, Formal analysis, Investigation, Writing-Original Draft preparation, Funding acquisition. V.F.-A.: Conceptualization, Validation, Supervision, Writing—Review and Editing, Project administration, Funding acquisition. S.C.A.: Conceptualization, Methodology, Validation, Writing—Review and Editing. All authors have read and agreed to the published version of the manuscript.

Funding: Carolina Gómez-Fontealba, Valentina Flores-Aqueveque and Stephane Alfaro were supported by Fondecyt grant no. 1191942; Carolina Gómez-Fontealba and Valentina Flores-Aqueveque were funded by National Agency for Research and Development (ANID)/Millennium Science Initiative/Millenium Nucleus Paleoclimate. Carolina Gómez-Fontealba is also funded by the ANID/Scolarship Program/Magister Nacional/2020-22210497. Valentina Flores-Aqueveque was also supported by IRD through CHARISMA Project (JE0ECCHARI).

Institutional Review Board Statement: Not applicable.

Informed Consent Statement: Not applicable.

Data Availability Statement: The meteorological station analyzed in this study were obtained from the Dirección Meteorológica de Chile (DMC) (https://www.meteochile.cl/ accessed on 30 April 2021), from Instituto de Investigaciones Agropecuarias (INIA) (https://agrometeorologia.cl/ accessed on 30 April 2021), and the data from the Torres del Paine station were facilitated by Dirección General de Aguas (DGA) (https://dga.mop.gob.cl/ accessed on 30 April 2021). Also, the data of ERA5 is available online at (https://cds.climate.copernicus.eu/ accessed on 30 April 2021), while dataset of MERRA-2 and GLDAS are available online at (https://giovanni.gsfc.nasa.gov/ accessed on 30 April 2021).

Acknowledgments: This research was funded by Fondecyt grant no. 1191942 from National Agency for Research and Development (ANID) and support of IRD. V.F.-A. acknowledges the support from IRD through CHARISMA Project (JE0ECCHARI). C.G.-F. and V.F.-A. would like to thank C. Gonzalez for his help in obtaining reanalysis data.

Conflicts of Interest: The authors declare no conflict of interest.

References

1. Garreaud, R.; Vuille, M.; Compagnucci, R.; Marengo, J. Present-day South American climate. *Palaeogeogr. Palaeoclimatol. Palaeoecol.* **2009**, *281*, 180–195. [CrossRef]
2. Kushner, P.; Held, I.; Delworth, T.L. Southern Hemisphere Atmospheric Circulation Response to Global Warming. *J. Clim.* **2001**, *14*, 2238–2249. [CrossRef]
3. Toggweiler, J.R. Shifting westerlies. *Science* **2009**, *323*, 1434. [CrossRef] [PubMed]
4. Garreaud, R.; Lopez, P.; Minvielle, M.; Rojas, M. Large-scale control on the Patagonian climate. *J. Clim.* **2013**, *26*, 215–230. [CrossRef]
5. Hodgson, D.A.; Sime, L.C. Southern westerlies and CO_2. *Nat. Geosci.* **2010**, *3*, 666–667. [CrossRef]
6. Moreno, P.; Videla, J.; Valero-Garcés, B.; Alloway, B.; Heusser, L. A continuous record of vegetation, fire-regime and climatic changes in northwestern Patagonia spanning the last 25,000 years. *Quat. Sci. Rev.* **2018**, *198*, 15–36. [CrossRef]
7. Stuut, J.-B.W.; Prins, M.A.; Schneider, R.R.; Weltje, G.J.; Jansen, J.H.F.; Postma, G. A 300-kyr record of aridity and wind strength in southwestern Africa: Inferences from grain-size distributions of sediments on Walvis Ridge, SE Atlantic. *Mar. Geol.* **2002**, *180*, 221–233. [CrossRef]
8. Flores-Aqueveque, V.; Alfaro, S.C.; Caquineau, S.; Foret, G.; Vargas, G.; Rutllant, J.A. Inter-annual variability of southerly winds in a coastal area of the Atacama Desert: Implications for the export of aeolian sediments to the adjacent marine environment. *Sedimentology* **2012**, *59*, 990–1000. [CrossRef]
9. Flores-Aqueveque, V.; Alfaro, S.; Vargas, G.; Rutllant, J.A.; Caquineau, S. Aeolian particles in marine cores as a tool for quantitative high-resolution reconstruction of upwelling favorable winds along coastal Atacama Desert, Northern Chile. *Prog. Oceanogr.* **2015**, *134*, 244–255. [CrossRef]
10. Bagnold, R.A. *The Physics of Blown Sand and Desert Dunes*; Chapman and Hall: London, UK, 2008; 265p.
11. Gelaro, R.; McCarty, W.; Suárez, M.; Todling, R.; Molod, A.; Tackacs, L.; Randles, C.; Darmenov, A.; Bosilovich, M.; Reichle, R.; et al. The Modern-Era Retrospective Analysis for Research and Applications, Version 2 (MERRA-2). *J. Clim.* **2017**, *30*, 5419–5454. [CrossRef]
12. Olauson, J. ERA5: The new champion of wind power modelling? *Renew. Energy* **2018**, *126*, 322–331. [CrossRef]
13. Hersbach, H.; Bell, B.; Berrisford, P.; Hirahara, S.; Horányi, A.; Muñoz Sabater, J.; Nicolas, J.; Peubey, C.; Radu, R.; Schepers, D.; et al. The ERA5 global reanalysis. *Q. J. R. Meteorol. Soc.* **2020**, *146*, 1999–2049. [CrossRef]

14. Browne, I.M.; Moy, C.M.; Riesselman, C.R.; Neil, H.L.; Curtin, L.G.; Gorman, A.R.; Wilson, G.S. Late Holocene intensification of the westerly winds at the subantarctic Auckland Islands (51° S), New Zealand. *Clim. Past* **2017**, *13*, 1301–1322. [CrossRef]
15. Valjarević, A.; Morar, C.; Živković, J.; Niemets, L.; Kićović, D.; Golijanin, J.; Gocić, M.; Bursać, N.M.; Stričević, L.; Žiberna, I.; et al. Long Term Monitoring and Connection between Topography and Cloud Cover Distribution in Serbia. *Atmosphere* **2021**, *12*, 964. [CrossRef]
16. Viale, M.; Bianchi, E.; Cara, L.; Ruiz, L.E.; Villalba, R.; Pitte, P.; Masiokas, M.; Rivera, J.; Zalazar, L. Contrasting Climates at Both Sides of the Andes in Argentina and Chile. *Front. Environ. Sci.* **2019**, *7*, 69. [CrossRef]
17. Sime, L.C.; Kohfeld, K.E.; Le Quéré, C.; Wolff, E.W.; de Boer, A.M.; Graham, R.M.; Bopp, L. Southern Hemisphere westerly wind changes during the Last Glacial Maximum: Model-data comparison. *Quat. Sci. Rev.* **2013**, *64*, 104–120. [CrossRef]
18. Lamy, F.; Kilian, R.; Arz, H.W.; Francois, J.P.; Kaiser, J.; Prange, M.; Steinke, T. Holocene changes in the position and intensity of the southern westerly wind belt. *Nat. Geosci.* **2010**, *3*, 695–699. [CrossRef]
19. Shindell, D.T.; Schmidt, G.A. Southern Hemisphere Climate Response to Ozone Changes and Greenhouse Gas Increases. *Geophys. Res. Lett.* **2004**, *31*, L18209. [CrossRef]
20. Sen Gupta, A.; Santoso, A.; Taschetto, A.S.; Ummenhofer, C.C.; Travena, J.; England, M.H. Projected Changes to the Southern Hemisphere Ocean and Sea Ice in the IPCC AR4 Climate Models. *J. Clim.* **2009**, *22*, 3047–3078. [CrossRef]
21. Thompson, D.W.; Solomon, S.; Kushner, P.J.; England, M.H.; Grise, K.M.; Karoly, D.J. Signatures of the Antarctic ozone hole in Southern Hemisphere surface climate change. *Nat. Geosci.* **2011**, *4*, 741. [CrossRef]
22. Thompson, D.W.J.; Wallace, J.M.; Hegerl, G.C. Annular modes in the extratropical circulation, Part II: Trends. *J. Clim.* **2000**, *13*, 1018–1036. [CrossRef]
23. Thompson, D.W.J.; Solomon, S. Interpretation of recent Southern Hemisphere climate change. *Science* **2002**, *296*, 895–899. [CrossRef]
24. Marshall, G.J.; Stott, P.A.; Turner, J.; Connolley, W.M.; King, J.C.; Lachlan-Cope, T.A. Causes of exceptional atmospheric circulation changes in the Southern Hemisphere. *Geophys. Res. Lett.* **2004**, *31*, L14205. [CrossRef]
25. Gillett, N.; Thompson, D. Simulation of Recent Southern Hemisphere Climate Change. *Science* **2003**, *302*, 273–275. [CrossRef] [PubMed]
26. Ihara, C.; Kushnir, Y. Change of mean midlatitude westerlies in 21st century climate simulations. *Geophys. Res. Lett.* **2009**, *36*, L13701. [CrossRef]
27. Fyfe, J.C.; Saenko, O.A. Simulated changes in the extratropical Southern Hemisphere winds and currents. *Geophys. Res. Lett.* **2006**, *33*, 06701. [CrossRef]
28. Chavaillaz, Y.; Codron, F.; Kageyama, M. Southern westerlies in LGM and future (RCP4.5) climates. *Clim. Past* **2013**, *9*, 517–524. [CrossRef]
29. Rodell, M.; Houser, P.R.; Jambor, U.; Gottschalck, J.; Mitchell, K.; Meng, C.-J.; Arsenault, K.; Cosgrove, B.; Radakovich, J.; Bosilovich, M.; et al. The Global Land Data Assimilation System. *Bull. Am. Meteorol. Soc.* **2004**, *85*, 381–394. [CrossRef]
30. European Centre for Medium-Range Weather Forecasts (ECMWF). ERA5 Back Extension 1950–1978 (Preliminary Version). Research Data Archive at the National Center for Atmospheric Research, Computational and Information Systems Laboratory. Available online: https://doi.org/10.5065/YBW7-YG52 (accessed on 20 April 2021).
31. Fécan, F.; Marticorena, B.; Bergametti, G. Parametrization of the increase of the Aeolian erosion threshold wind friction velocity due to soil moisture for arid and semi-arid areas. *Ann. Geophys.* **1999**, *17*, 149–157. [CrossRef]
32. Ishizuka, M.; Mikami, M.; Yamada, Y.; Zeng, F.; Gao, W. An observational study of soil moisture effects on wind erosion at a gobi site in the Taklimakan Desert. *J. Geophys. Res. Atmos.* **2005**, *110*, 18. [CrossRef]
33. Alfaro, S.C.; Gomes, L. Improving the large-scale modeling of the saltation flux of soil particles in presence of nonerodible elements. *J. Geophys. Res. Atmos.* **1995**, *100*, 16357–16366. [CrossRef]
34. Marticorena, B.; Bergametti, G. Modeling the atmospheric dust cycle: 1. Design of a soil-derived dust emission scheme. *J. Geophys. Res. Atmos.* **1995**, *100*, 16415–16430. [CrossRef]
35. Flores-Aqueveque, V.; Rojas, M.; Aguirre, C.; Arias, P.; González, C. South Pacific Subtropical High from the late Holocene to the end of the 21st century: Insights from climate proxies and general circulation models. *Clim. Past* **2020**, *16*, 79–99. [CrossRef]
36. Santana, A.; Olave, C.; Butorovic, N. Climate study high temporal resolution records in camp Posesion (ENAP). Magallanes, Chile. *An. Inst. Patagon.* **2010**, *38*, 5–34. [CrossRef]
37. Ramon, J.; Lledó, L.; Torralba, V.; Soret, A.; Doblas-Reyes, F.J. What global reanalysis best represents near-surface winds? *Q. J. R. Meteorol. Soc.* **2019**, *145*, 3236–3251. [CrossRef]
38. Tetzner, D.; Thomas, E.R.; Allen, C.S. A Validation of ERA5 Reanalysis Data in the Southern Antarctic Peninsula—Ellsworth Land Region, and Its Implications for Ice Core Studies. *Geosciences* **2019**, *9*, 289. [CrossRef]
39. Pérez-Santos, I.; Seguel, R.; Schneider, W.; Linford, P.; Donoso, D.; Navarro, E.; Amaya-Cárcamo, C.; Pinilla, E.; Daneri, G. Synoptic-scale variability of surface winds and ocean response to atmospheric forcing in the eastern austral Pacific Ocean. *Ocean Sci.* **2019**, *15*, 1247–1266. [CrossRef]
40. Guozden, T.M.; Bianchi, E.; Solarte, A.; Mulleady, C. Wind resource assessment in the Rio Negro province (Patagonia Argentina) using MERRA Reanalysis. *Meteorologica* **2017**, *43*, 47–61.
41. Marshall, G.J. Trends in the Southern Annular Mode from Observations and Reanalyses. *J. Clim.* **2003**, *16*, 4134–4143. [CrossRef]
42. Cane, M.A. Climate change—A role for the tropical Pacific. *Science* **1998**, *282*, 59–61. [CrossRef]

43. Dettinger, M.D.; Battisti, D.S.; Garreaud, R.D.; McCabe, G.J.; Bitz, C.M. Interhemispheric Effects of Interannual and Decadal ENSO-Like Climate Variations on the Americas. In *Interhemispheric Climate Linkages: Present and Past Climates in the Americas their Societal Effects*; Markgraf, V., Ed.; Academic Press: Cambridge, MA, USA, 2001; pp. 1–16.
44. Cane, M.A. The evolution of El Niño, past and future. *Earth Planet. Sci. Lett.* **2005**, *230*, 227–240. [CrossRef]
45. Thompson, D.W.J.; Wallace, J.M. Annular modes in the extratropical circulation, Part I: Month-to-month variability. *J. Clim.* **2000**, *13*, 1000–1016. [CrossRef]
46. Swart, N.C.; Fyfe, J.C. Observed and simulated changes in the Southern Hemisphere surface westerly wind-stress. *Geophys. Res. Lett.* **2012**, *39*, 16711. [CrossRef]
47. Mantua, N.J.; Hare, S.R.; Zhang, Y.; Wallace, J.M.; Francis, R.C. A Pacific interdecadal climate oscillation with impacts on salmon production. *Bull. Am. Meteorol. Soc. Bull. Am. Meteorol. Soc.* **1997**, *78*, 1069–1079. [CrossRef]
48. Mantua, N.J.; Hare, S.R. The Pacific Decadal Oscillation. *J. Oceanogr.* **2002**, *58*, 35–44. [CrossRef]
49. Garreaud, R.D.; Battisti, D.S. Interannual (ENSO) and interdecadal (ENSO-like) variability in the Southern Hemisphere tropospheric circulation*. *J. Clim.* **1999**, *12*, 2113–2123. [CrossRef]
50. Bertrand, S.; Hughen, K.; Sepúlveda, J.; Pantoja, S. Late Holocene covariability of the southern westerlies and sea surface temperature in northern Chilean Patagonia. *Quat. Sci. Rev.* **2014**, *105*, 195–208. [CrossRef]
51. Lamy, F.; Hebbeln, D.; Röhl, U.; Wefer, G. Holocene rainfall variability in southern Chile: A marine record of latitudinal shifts of the Southern Westerlies. *Earth Planet Sci. Lett.* **2001**, *185*, 369–382. [CrossRef]
52. Moy, C.M.; Dunbar, R.B.; Moreno, P.I.; François, J.P.; Villa- Martínez, R.; Mucciarone, D.M.; Guilderson, T.O.; Garreaud, R. Isotopic evidence for hydrologic change related to the westerlies in SW Patagonia, Chile, during the last millennium. *Quat. Sci. Rev.* **2008**, *27*, 1335–1349. [CrossRef]
53. Varma, V.; Prange, M.; Merkel, U.; Kleinen, T.; Lohmann, G.; Pfeiffer, M.; Renssen, H.; Wagner, A.; Wagner, S.; Schulz, M. Holocene evolution of the Southern Hemisphere westerly winds in transient simulations with global climate models. *Clim. Past* **2012**, *8*, 391–402. [CrossRef]
54. Henriquez, W.I.; Villa-Martinez, R.; Vilanova, I.; De Pol-Holz, R.; Moreno, P.I. The last glacial termination on the eastern flank of the central Patagonian Andes (47° S). *Clim. Past* **2017**, *13*, 879–895. [CrossRef]